Publ. Astron. Soc. Japan (2020) 72 (6), 99 (1–5)
doi: 10.1093/pasj/psaa097
Advance Access Publication Date: 2020 October 21

Gaia DR2 data and the evolutionary status of eight high-velocity hot post-AGB candidates

Mudumba Parthasarathy,[1,2] Tadafumi Matsuno,[3,†] and Wako Aoki[2,3,*]

[1]Indian Institute of Astrophysics, II Block, Koramangala, Bangalore 560 034, India
[2]National Astronomical Observatory, 2-21-1 Osawa, Mitaka, Tokyo 181-8588, Japan
[3]Department of Astronomical Science, School of Physical Sciences, The Graduate University of Advanced Studies (SOKENDAI), 2-21-1 Osawa, Mitaka, Tokyo 181-8588, Japan

*E-mail: aoki.wako@nao.ac.jp
†Present address: Kapteyn Astronomical Institute, University of Groningen, Landleven 12, 9747 AD Groningen, The Netherlands

Received 2020 August 7; Accepted 2020 September 28

Abstract

From Gaia DR2 data of eight high-velocity hot post-AGB candidates, LS 3593, LSE 148, LS 5107, HD 172324, HD 214539, LS IV −12 111, LS III +52 24, and LS 3099, we found that six of them have accurate parallaxes which made it possible to derive their distances, absolute visual magnitudes (M_V) and luminosity ($\log L/L_\odot$). All the stars except LS 5107 have an accurate effective temperature ($T_{\rm eff}$) in the literature. Some of these stars are metal poor, and some of them do not have circumstellar dust shells. In the past, the distances of some stars were estimated to be 6 kpc, which we find to be incorrect. The accurate Gaia DR2 parallaxes show that they are relatively nearby, post-AGB stars. When compared with post-AGB evolutionary tracks we find their initial masses to be in the range 1 $M_\odot$ to 2 $M_\odot$. We find the luminosity of LSE 148 to be significantly lower than that of post-AGB stars, suggesting that this is a post-horizontal-branch star or post-early-AGB star. LS 3593 and LS 5107 are new high-velocity hot post-AGB stars from Gaia DR2.

Key words: stars: AGB and post-AGB — stars: distances — stars: evolution — stars: high-velocity

1 Introduction

Hot post-AGB stars are transition objects evolving towards the early stages of planetary nebulae (see Kwok 1993; Parthasarathy et al. 1993, 1995; van Winckel 2003; Parthasarathy 2006, and references therein). Some of the hot post-AGB stars are at high galactic latitudes and a few are high-velocity stars, e.g., LS III +52 24 (IRAS 22023+5249: $V_r = -148\,{\rm km\,s^{-1}}$; Sarkar et al. 2012), LS 5112 (IRAS 18379−1707: $V_r = -124\,{\rm km\,s^{-1}}$; Ikonnikova et al. 2020). These stars could be highly evolved low-mass metal-poor stars in the halo population of the Milky Way. Determination of the evolutionary status and frequency of these objects is useful for better understanding of both low-mass star evolution and the Milky Way halo structure.

Hence, these objects prompted us to look for more such stars. However the radial velocities and distances of most hot post-AGB candidates were not available. With the advent of Gaia DR2 data (Gaia Collaboration 2018; Lindegren et al. 2018) one can look for more such stars.

We considered the hot post-AGB candidates given in the following papers: Przybylski (1969); Kendall et al. (1994); Venn et al. (1998); Sarkar, Parthasarathy, and Reddy (2005); Sarkar et al. (2012); Mello et al. (2012);

Table 1. Stars under consideration.

Object	l (°)	b (°)	Parallax (p) (mas)	V_r (km s^{-1})	G (mag)	V (mag)	$B-V$ (mag)	Spectral type	Note
LS 3593	330.6439866	−3.672106351	0.410 ± 0.047	110.12 ± 1.94	9.44	9.53	0.15	B8Iab	
LSE 148	355.54719	−20.42079462	0.697 ± 0.106	−134.00 ± 4.30	10.15	10.17	−0.20	B6Ib	
LS 5107	19.24285127	−3.663147838	0.624 ± 0.052	−76.65 ± 8.30	9.52	9.89	0.86	B9Iae	V452 Sct IRAS source
HD 172324	66.18384285	18.58124629	0.456 ± 0.042	−117.10 ± 2.00	8.14	8.16	0.01	A0Iabe	V534 Lyr
HD 214539	319.7541249	−44.93459676	0.719 ± 0.041	333.00 ± 2.80	7.18	7.25	0.00	B9Ib/A0Iab	
LS 3099	308.3016934	6.35580537	0.377 ± 0.050	65.31 ± 0.34	10.70	10.68	0.39	B1Iae	IRAS source
LS IV −12 111	29.17960346	−21.2637799	0.129 ± 0.055:	86.9 ± 1.7	11.32	11.4	−0.1	B1Iae	IRAS source
LS III +52 24	99.30346632	−1.955656239	0.080 ± 0.052:	−148.31 ± 0.60	12.36	12.51	0.72	B1I	IRAS source

Table 2. Distance and stellar parameters.

Object	Distance (D) (pc)	$E(B-V)$ (mag)	$E(B-V)_{sp}$ (mag)	M_V (mag)	M_g (mag)	$\log L/L_\odot$	T_{eff} (K)	$\log g$	[Fe/H]	References*
LS 3593	2436 ± 281	0.21	0.18	−2.97	−3.07 ± 0.26	3.35 ± 0.11	9300	1.7	−2.0	1
LSE 148	1436 ± 219	0.10	0.07	−0.08	−0.91 ± 0.34	2.59 ± 0.14	30900	3.8	<−2.0	2
LS 5107	1602 ± 135	0.56	0.88	−2.64	−3.04 ± 0.19	3.17 ± 0.09	10500	2.0	—	
HD 172324	2194 ± 202	0.06	0.02	−3.71	−3.73 ± 0.21	3.54 ± 0.09	10000	2.5	−0.3	3
HD 214539	1392 ± 80	0.03	0.02	−3.55	−3.62 ± 0.14	3.53 ± 0.07	9800	1.6	<−1.5	4, 5
LS 3099	2650 ± 351	0.33	0.51	−3.12	—	3.67 ± 0.12	20200	2.38		
LS IV −12 111	>4180	0.19	0.28	<−2.32	<−2.32	>3.63	20500	2.5		
LS III 52-24	>5398	0.67	0.64	<−2.95	<−3.14	>3.92	24000	3.0		

*References: 1 Venn et al. (1998); 2 Mello et al. (2012); 3 Klochkova, Sendzikas, and Chentsov (2018); 4 Kodaira and Philip (1984); 5 Przybylski (1969).

and Klochkova, Sendzikas, and Chentsov (2018). From the Gaia DR2 data we found LS 3593 (SAO 243754), LSE 148 (HD 177566), LS 5107 (IRAS 18365−1353), HD 172324 (V 534 Lyr), HD 214539, and LS 3099 to be high-velocity stars with accurate Gaia DR2 parallaxes (see tables 1 and 2). LS IV −12 111 and LS III +52 24 do not have accurate parallaxes. We also looked at the proper motion data of these eight stars in Gaia DR2.

In this paper we analyze the Gaia DR2 data of the above-mentioned eight stars, and based on this we discuss their evolutionary status.

2 Data and analysis

The Galactic longitude and latitude, parallaxes, radial velocities, G (Gaia G band), V, $B-V$, and spectral types of the eight stars mentioned above are given in table 1. The data are taken from SIMBAD and Gaia DR2.

The distances to the stars are derived using the Gaia DR2 parallaxes (table 2). The $E(B-V)$ values (table 2) are obtained from Schlegel, Finkbeiner, and Davis (1998) for the high-galactic-latitude stars (LSE 148, HD 172324, HD 214539). The interstellar reddening of these three stars is quite small. Chen et al. (2019) and Green et al. (2018) are used for LS 3593 and LS 5107, respectively. Extinction coefficients are converted using values provided in Green et al. (2018) and Schlafly and Finkbeiner (2011), and mean values in Casagrande and VandenBerg (2018). Table 2 lists $E(B-V)$ obtained from the dust map as well as $E(B-V)$ values calculated from the observed $(B-V)$ and intrinsic $(B-V)$ obtained from their spectral types $[E(B-V)_{sp}]$. The $E(B-V)_{sp}$ values of the three IRAS sources are 0.09–0.32 mag larger than the $E(B-V)$ estimated from the dust map. This suggests that they are affected by circumstellar reddening, in addition to the interstellar reddening.

The calculated absolute visual magnitudes M_V are given in table 2. For the M_V values we applied bolometric corrections as the T_{eff} values and spectral types of all the stars are well determined. The bolometric corrections were taken from Cox (2000). The values of the bolometric corrections in Flower (1996) are 0.1–0.25 mag larger than those of Cox (2000), resulting in differences in $\log L/L_\odot$ of less than 0.1 dex. This does not affect the discussion on the nature of our high-velocity post-AGB stars. The derived bolometric magnitudes M_{bol} and $\log L/L_\odot$ values are given in table 2. Notes on all eight stars are given below.

The stellar parameters, i.e., T_{eff}, $\log g$, and [Fe/H], are given in table 2. Details of these parameters and references will be provided for the individual objects below.

Kinematics are calculated using Gaia parallax and proper motion measurements. We adopt 8.2 kpc as the distance between the Sun and the Galactic center (McMillan

Table 3. Kinematics data.

Object	μ_α (mas)	$\sigma(\mu_\alpha)$ (mas)	μ_δ (mas)	$\sigma(\mu_\delta)$ (mas)	V_R (km s^{-1})	$\sigma(V_R)$ (km s^{-1})	V_ϕ (km s^{-1})	$\sigma(V_\phi)$ (km s^{-1})	V_Z (km s^{-1})	$\sigma(V_Z)$ (km s^{-1})
LS 3593	−4.252	0.066	−11.621	0.053	−56.85	7.44	78.13	11.73	−56.17	6.27
LSE 148	−2.030	0.167	−42.817	0.157	163.10	7.89	−8.18	34.46	−17.97	10.04
LS 5107	−4.487	0.082	−6.045	0.074	−83.46	7.52	228.88	4.71	11.15	0.83
HD 172324	−3.183	0.079	−0.969	0.080	68.09	3.74	144.65	2.31	−61.38	3.23
HD 214539	−25.891	0.057	−26.177	0.065	−320.38	7.23	−31.02	8.53	−63.93	9.96
LS 3099	−5.69	0.074	−2.744	0.079	−39.7	2.0	146.7	5.1	−6.9	3.2
LS IV −12 111	−3.596	0.094	−4.096	0.061						
LS III 52-24	−3.856	0.100	−2.566	0.070						

2017), and 0.025 kpc as the vertical offset of the Sun (Jurić et al. 2008). Solar motion is adopted from Schönrich, Binney, and Dehnen (2010) for the radial and vertical velocities (11.1 km s^{-1} and 7.25 km s^{-1}, respectively) and is calculated as 247.97 km s^{-1} using the proper motion measurements by Reid and Brunthaler (2004). The results are presented in table 3.

From the radial velocity measurements by previous studies, no clear signature of binarity has been found for these stars. The constraint is still not very strong due to the limitation of the number of spectroscopic observations. We note that the sample selection of high-velocity post-AGB stars would not be affected if they belong to low-mass binaries because the radial velocity variations expected for low-mass binaries are not as large as the radial velocity of the stars studied in this paper.

2.1 Notes on the eight stars

2.1.1 LS 3593

Venn et al. (1998) derived $T_{\rm eff} = 9300$ K, $\log g = 1.7$, and found the chemical composition of this star to be metal poor ([Fe/H] = −2.0). Oxygen and nitrogen seem to be slightly overabundant. They did not find any emission lines in the spectrum, and they found it to be a very slow rotator. Its galactic latitude is low but it is found to be a high-velocity star.

2.1.2 LSE 148

This is a high-galactic-latitude and high-velocity star (table 1). Kendall et al. (1994) derived $T_{\rm eff} = 30600$ K and $\log g = 3.5$, and found it to be metal poor. Carbon is underabundant, similar to that observed in high-galactic-latitude hot post-AGB stars. They concluded that it is a hot post-AGB star of core mass 0.55 $M_\odot$, and found it to be a very slow rotator. No emission lines are present in the spectrum. Mello et al. (2012) also found it to be very metal poor. They found weak emission in the cores of Balmer lines. Mello et al. (2012) derived $T_{\rm eff} = 30900$ K and $\log g = 3.8$, which agrees well with the results obtained by Kendall et al. (1994). Mello et al. (2012) found no Fe lines in the spectrum of LSE 148. They suggested that it may be a post-horizontal-branch star or a post-early-AGB star. This is supported by the present work with a much more robust estimate of the luminosity (see section 3).

2.1.3 LS 5107 (IRAS 18365−1353)

There is no detailed study of the spectrum of this star. Venn et al. (1998) found the Hα line to be a P-Cygni profile and the FeII emission line at 6515 Å. LS 5107 is found to be an IRAS source with far-IR colors similar to post-AGB stars and planetary nebulae. The $T_{\rm eff}$ given in table 2 is estimated from its spectral type. We conclude that LS 5107 is a high-velocity hot post-AGB star.

2.1.4 HD 172324 (V534 Lyr)

This is a high-galactic-latitude and high-velocity star (table 1). It is a small-amplitude light and radial velocity variable. Recently, Klochkova, Sendzikas, and Chentsov (2018) made a detailed analysis of high-resolution spectra of this star and derived its chemical composition. They found $T_{\rm eff} = 10000$ K, $\log g = 2.5$, and that it is metal poor and overabundant in nitrogen. The Hα line shows a variable P-Cygni profile. They concluded that it is a Population II pulsating star near the horizontal branch. Klochkova, Sendzikas, and Chentsov (2018) derived a distance of 6 kpc, whereas Bonsack and Greenstein (1956) estimated a distance of 5.7 kpc. The Gaia DR2 data (tables 1 and 2), however, clearly shows that their distance estimate is wrong. The luminosity estimated from this distance is much higher than the value expected for horizontal-branch stars. We note that the $\log g$ value derived by the spectroscopic analysis of Klochkova, Sendzikas, and Chentsov (2018) is also lower than the typical values of horizontal-branch stars.

2.1.5 HD 214539

This is a high-galactic-latitude and very-high-velocity star (table 1). Przybylski (1969) made a detailed analysis of the spectrum of this star, and found it to be a metal-poor

([Fe/H] = −1.2) and low-gravity star. It was considered at that time the brightest known blue-halo star. Kodaira and Philip (1984) derived $T_{\rm eff} = 9800$ K and $\log g = 1.6$.

2.1.6 LS 3099 (IRAS 13266−5551)

Mello et al. (2012) and Sarkar, Parthasarathy, and Reddy (2005) analyzed the high-resolution spectrum of this B1 Iae post-AGB star. They found $T_{\rm eff} = 20200$ K, $\log g = 2.38$, and that it is mildly carbon poor and metal poor (Mello et al. 2012). The radial velocity was found to be $65.31 \pm 0.34\,{\rm km\,s^{-1}}$ (Sarkar et al. 2005).

2.1.7 LS IV −12 111 (IRAS 19590−1249)

This is a high-galactic-latitude ($b = -21.^{\circ}26$) and high-velocity ($86.9\,{\rm km\,s^{-1}}$) hot (B1 Iae) post-AGB star. Ryans et al. (2003) and Mello et al. (2012) analyzed the high-resolution spectrum of this star, and derived $T_{\rm eff} = 20500$ K and $\log g = 2.5$ (Ryans et al. 2003); the values derived by Mello et al. (2012) are in agreement with the results of Ryans et al. (2003). They found it to be carbon poor by ∼0.4 dex, similar to high-galactic-latitude OB post-AGB stars, indicating that the star left the AGB before the third dredge-up. The parallax of this object in Gaia DR2 is not sufficiently accurate.

2.1.8 LS III +52 24 (IRAS 22023+5249)

Sarkar et al. (2012) analyzed the high-resolution spectrum of this hot (B1 I) post-AGB star, and found the radial velocity to be $-148.31 \pm 0.60\,{\rm km\,s^{-1}}$, $T_{\rm eff} = 24000 \pm 1000$ K, $\log g = 3.0 \pm 0.5$, and that it is metal poor at −0.12 dex. The spectrum shows nebular emission lines, indicating the presence of a low-excitation planetary nebula. Arkhipova et al. (2013) found small-amplitude light variations similar to other post-AGB stars. The parallax of this object in Gaia DR2 is not sufficiently accurate.

3 Discussion

We show in figure 1 the location of six high-velocity stars in the Hertzsprung–Russell diagram. The LS IV −12 111 and LS III +52 24 parallaxes were not determined within an accuracy of three sigma, and hence are not shown in figure 1. Four of the six stars have similar $T_{\rm eff}$ and L along the evolutionary tracks of low-mass post-AGB stars.

Kinematics show that all the stars except LS 5107 do not follow the Galactic rotation. LS 5107, for which there is no estimate of metallicity, could belong to the thin disk, according to the kinematics information. LSE 148 and HD 214539 show large velocities relative to the Sun, and hence they would belong to the Galactic halo, indicating that their initial masses are low. The other three, LS 3593, HD 172324, and LS 3099, show modest relative velocities

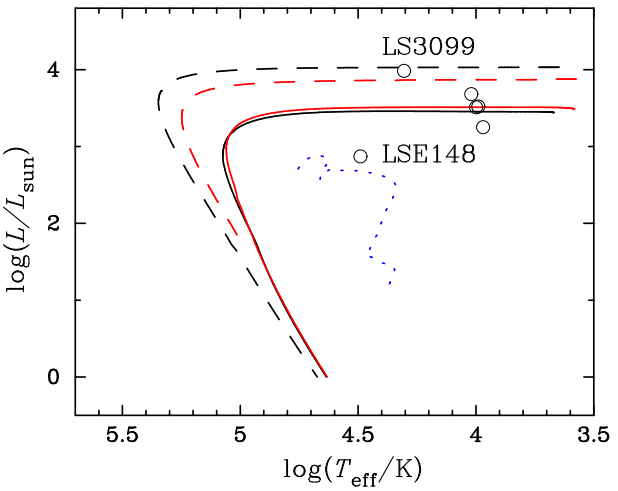

Fig. 1. Evolutionary tracks of post-AGB phases taken from Miller Bertolami (2016) for initial masses of 1.0 $M_\odot$ (solid lines) and 2.0 $M_\odot$ (dotted lines) with $Z = 0.02$ (red) and $Z = 0.001$ (black). The evolutionary track of a post-horizontal-branch star with a core mass of 0.52 $M_\odot$ with [Fe/H] = −1.48 taken from Dorman, Rood, and O'Connell (1993) is shown by the dotted (blue) line. The six objects studied in the present work are shown by open circles. (Color online)

compared to the Sun. Although they could belong to the Galactic disk, it is unlikely that their ages are young given the age–velocity dispersion relation among Milky Way disk stars (e.g., Casagrande et al. 2011). These kinematic features are consistent with the results from the positions in the $T_{\rm eff}$–$\log L$ plane that these stars are low-mass halo post-AGB objects.

LSE 148 has a luminosity that is even lower than low-mass post-AGB stars. This suggests that it is a post-horizontal-branch star or a post-early-AGB star.

LS 3099 has a luminosity similar to post-AGB stars whose initial mass was about 2.0 $M_\odot$ (figure 1), and is not metal poor. This star may be a thick-disk star with relatively high metallicity.

Although LS IV −12 111 and LS III +52 24 do not have reliable parallax measurements, we can place lower limits on their tangential velocities. The 2 σ lower limits are 108 ($\rm km\,s^{-1}$) and 118 ($\rm km\,s^{-1}$), respectively. These results, together with their large radial velocities, support that these are high-velocity stars.

3.1 Frequency of metal-poor post-AGB stars and timescale of evolution

We find four metal-poor post-AGB stars with low core masses (∼0.55 $M_\odot$, which corresponds to initial masses of 1.0 $M_\odot$ or smaller). They have $T_{\rm eff} \sim 10000$ K. Taking account of the incompleteness of the sample of this study, this can be used to estimate the lower limit of the frequency of such objects in the Galaxy. The distances of these objects

are about 2 kpc or less, which became available thanks to Gaia DR2 for the first time. The local stellar density of the halo structure is estimated to be 3–15 $\times$ 10^{-5} $M_{\odot}$ pc^{-3} (Deason et al. 2019 and references therein). Adopting the recent estimate of 7×10^{-5} $M_{\odot}$ pc^{-3} in Deason, Belokurov, and Sanders (2019), the stellar halo mass within 2 kpc is 1.7×10^{6} $M_{\odot}$. Hence, the frequency of metal-poor post-AGB stars is of the order of 10^{-6}. If a higher luminosity (larger distance) was applied, as estimated by previous studies for some of our post-AGB stars, the frequency could be much lower. Taking account of the lifetime of such low-mass stars ($\sim 10^{10}$ yr), the timescale of the evolution in this phase is estimated to be 10^{4} yr. This roughly agrees with the prediction of the recent model calculation of Miller Bertolami (2016) shown in their figure 8 for metal-poor low-mass stars.

Since the timescale of the evolution of low-mass metal-poor objects is even longer from 10000 K to the maximum effective temperature ($\sim$100000 K), hotter high-velocity post-AGB stars with low metallicity could exist in the Milky Way halo that are not yet identified. Further searches for such stars will provide useful constraints on the frequency of low-mass metal-poor post-AGB stars.

Acknowledgments

MP was supported by the NAOJ Visiting Fellow Program of the Research Coordination Committee, National Astronomical Observatory of Japan (NAOJ), National Institutes of Natural Sciences (NINS). This work has made use of data from the European Space Agency (ESA) mission Gaia (https://www.cosmos.esa.int/gaia), processed by the Gaia Data Processing and Analysis Consortium (DPAC; https://www.cosmos.esa.int/web/gaia/dpac/consortium). Funding for the DPAC has been provided by national institutions, in particular the institutions participating in the Gaia Multilateral Agreement.

References

Arkhipova, V. P., Burlak, M. A., Esipov, V. F., Ikonnikova, N. P., & Komissarova, G. V. 2013, Astron. Lett., 39, 619
Bonsack, W. K., & Greenstein, J. L. 1956, PASP, 68, 249
Casagrande, L., Schönrich, R., Asplund, M., Cassisi, S., Ramírez, I., Meléndez, J., Bensby, T., & Feltzing, S. 2011, A&A, 530, A138
Casagrande, L., & VandenBerg, D. A. 2018, MNRAS, 479, L102
Chen, B.-Q., et al. 2019, MNRAS, 483, 4277
Cox, A. N. ed. 2000, Allen's Astrophysical Quantities, 4th ed. (New York: Springer)
Deason, A. J., Belokurov, V., & Sanders, J. L. 2019, MNRAS, 490, 3426
Dorman, B., Rood, R. T., & O'Connell, R. W. 1993, ApJ, 419, 596
Flower, P. J. 1996, ApJ, 469, 355
Gaia Collaboration 2018, A&A, 616, A1
Green, G. M., et al. 2018, MNRAS, 478, 651
Ikonnikova, N. P., Parthasarathy, M., Dodin, A. V., Hubrig, S., & Sarkar, G. 2020, MNRAS, 491, 4829
Jurić, M., et al. 2008, ApJ, 673, 864
Kendall, T. R., Brown, P. J. F., Conlon, E. S., Dufton, P. L., & Keenan, F. P. 1994, A&A, 291, 851
Klochkova, V. G., Sendzikas, E. G., & Chentsov, E. L. 2018, Astrophys. Bull., 73, 52
Kodaira, K., & Philip, A. G. D. 1984, ApJ, 278, 208
Kwok, S. 1993, ARA&A, 31, 63
Lindegren, L., et al. 2018, A&A, 616, A2
McMillan, P. J. 2017, MNRAS, 465, 76
Mello, D. R. C., Daflon, S., Pereira, C. B., & Hubeny, I. 2012, A&A, 543, A11
Miller Bertolami, M. M. 2016, A&A, 588, A25
Parthasarathy, M. 2006, in IAU Symp. 234, Planetary Nebulae in our Galaxy and Beyond, ed. M. J. Barlow & R. H. Méndez (Cambridge: Cambridge University Press), 79
Parthasarathy, M., et al. 1995, A&A, 300, L25
Parthasarathy, M., Garcia-Lario, P., Pottasch, S. R., Manchado, A., Clavel, J., de Martino, D., van de Steene, G. C. M., & Sahu, K. C. 1993, A&A, 267, L19
Przybylski, A. 1969, MNRAS, 146, 71
Reid, M. J., & Brunthaler, A. 2004, ApJ, 616, 872
Ryans, R. S. I., Dufton, P. L., Mooney, C. J., Rolleston, W. R. J., Keenan, F. P., Hubeny, I., & Lanz, T. 2003, A&A, 401, 1119
Sarkar, G., García-Hernández, D. A., Parthasarathy, M., Manchado, A., García-Lario, P., & Takeda, Y. 2012, MNRAS, 421, 679
Sarkar, G., Parthasarathy, M., & Reddy, B. E. 2005, A&A, 431, 1007
Schlafly, E. F., & Finkbeiner, D. P. 2011, ApJ, 737, 103
Schlegel, D. J., Finkbeiner, D. P., & Davis, M. 1998, ApJ, 500, 525
Schönrich, R., Binney, J., & Dehnen, W. 2010, MNRAS, 403, 1829
van Winckel, H. 2003, ARA&A, 41, 391
Venn, K. A., Smartt, S. J., Lennon, D. J., & Dufton, P. L. 1998, A&A, 334, 987